



ARTICLE

CFD Modeling to Evaluate User Safety by Using Flame Retardants in Asphalt Road Pavements during Large Tunnel Fires

Ciro Caliendo, Isidoro Russo* and Gianluca Genovese

Department of Civil Engineering, University of Salerno, via Giovanni Paolo II, 132, Fisciano, 84084, Salerno, Italy

*Corresponding Author: Isidoro Russo. Email: isrusso@unisa.it

Received: 21 May 2025; Accepted: 03 July 2025; Published: 31 July 2025

ABSTRACT: Road pavements in tunnels are usually made of asphalt mixtures, which, unfortunately, are flammable materials. Hence, this type of pavement could release heat, and more specifically smoke, in the event of a tunnel fire, thereby worsening the environmental conditions for human health. Extensive research has been conducted in recent years to enhance the fire reaction of traditional asphalt mixtures for the road pavements used in tunnels. The addition of the Flame Retardants (FRs) in conventional asphalt mixtures appears to be promising. Nevertheless, the potential effects of the FRs in terms of the reduction in consequences on tunnel users in the event of a large fire do not seem to have been sufficiently investigated by using fluid dynamics analysis as a computational tool. Given this gap of knowledge, this article aims to quantitatively evaluate whether the use of flame-retarded asphalt mixtures, as opposed to traditional ones without FRs, might mitigate the adverse effects on the safety of evacuees and fire brigade by performing numerical analyses in the case of a tunnel fire. To achieve this goal, 3D Computational Fluid Dynamics (CFD) models, which were executed using the Fire Dynamics Simulator (FDS) tool, were established in the case of a major fire of a Heavy Goods Vehicle (HGV) characterized by a maximum Heat Release Rate (HRR_{max}) of 100 MW. The people evacuation process was also simulated, and the Evac tool was used. Compared to the traditional asphalt pavements without FRs, the simulation findings indicated that the addition of the FRs causes a reduction in CO and CO₂ levels in the tunnel during the aforementioned fire, with a minor number of evacuees being exposed to the risk of incapacity to self-evacuate, as well as certain safety benefits for the operability of the firefighters entering the tunnel downstream of the fire when the tunnel is naturally ventilated.

KEYWORDS: Asphalt pavement combustion; flame retardants; road tunnel fire; CFD modeling; user safety; operability of fire brigade

1 Introduction

In tunnel fire safety, the impact of road pavement burning on the development of fire and its consequences has often been overlooked. The focus has generally been on how to preserve the functionality of structural elements and safety equipment, such as extinguishing and ventilation systems, when subjected to a fire, together with the process by which occupants leave these structures during such emergencies. Likewise, the European Directive 2004/54/EC [1], transposed into Italian law in 2006 [2], does not address the influence of the road pavement in the case of tunnel fires, focusing, in addition to user safety, solely on the fire performance of the structural components and equipment.

Given their low noise, good skid resistance, and ease of maintenance, flexible pavements composed of traditional asphalt mixtures are generally used in road tunnels compared to rigid pavements consisting of



jointed cement concrete. Nevertheless, asphalt mixtures might ignite when exposed to heat fluxes such as those resulting from a Heavy Goods Vehicle (HGV) fire [3], thereby releasing heat and toxic substances dangerous to humans. According to a recent study [4], during a large tunnel fire, the burning of traditional asphalt pavement can elevate smoke levels within the tunnel, thus increasing the likelihood that occupants cannot self-evacuate safely.

Since the combustion of traditional asphalt mixtures can, therefore, represent an additional issue when a large fire occurs in a tunnel, there is evidence that their fire reaction should be improved. Various types of Flame Retardants (FRs) might be added to asphalt mixtures. Compared with conventional ones without FRs, flame-retarded asphalt mixtures may present reduced flammability, resulting in improved flame retardancy (i.e., a higher ignition time and temperature (T_{ignition}), which are the time and temperature when the road surface could start to burn in the event of a fire), as well as result in reduced releases of both heat and smoke once ignited [5].

Several studies, mainly through laboratory tests, have assessed the positive effects of adding FRs to traditional asphalt mixtures of road pavements. By performing cone calorimeter tests to study the combustion characteristics of different asphalt mixtures containing or not FRs when subjected to fire conditions, numerous studies have proved that asphalt mixtures including FRs generally exhibit both a reduced heat release [6,7] and amount of smoke [8,9], CO [3,10,11], and CO₂ [5,12,13] emitted, together with a greater value of the T_{ignition} and delayed ignition time [14,15]. A literature review on the properties, toughness, and tensile strength of composites with different FRs may be found in Gupta et al. [16], as well as the effect of incorporating the ammonium polyphosphate as a flame retardant on the mechanical and viscoelastic properties is evaluated in Singh et al. [17].

The aforementioned studies are all based on laboratory tests. Whereas the tool of numerical modeling based on a fluid dynamics analysis to evaluate the beneficial impact of flame retardants on user safety during large road tunnel fires appears to be insufficiently explored. The present paper intends to fill this gap.

This study aims to quantitatively assess by means of numerical simulations whether the use of flame-retarded asphalt mixtures, as opposed to the traditional ones without FRs, might contribute to alleviating the negative impact on the safety of users and fire brigade because of the combustion of the road pavement during a large fire inside a tunnel. Tunnel fire simulations based on 3D Computational Fluid Dynamics (CFD) modeling are set up and carried out with the Fire Dynamics Simulator (FDS) code [18], while the related occupant evacuation process is replicated with the Evac tool [19]. The road tunnel under examination is assumed to be 900 m long. It is characterized by congested bi-directional traffic when a large fire involving an HGV, identified by a maximum Heat Release Rate (HRR_{max}) of 100 MW, occurs within the structure. For making a comparison, the road tunnel investigated is also assumed to be either mechanically or naturally ventilated. It is important to emphasize that the primary objective of this study is not to model the detailed combustion process of asphalt mixtures, but rather to evaluate the impact of their burning on user safety during fire events in road tunnels.

Regarding the organization of the article, the description of the road tunnel being examined, along with the fire and escape scenarios, is included in the next section. This is followed by a presentation of the proposed 3D CFD and evacuation modeling. Considering both cases of a road pavement made of asphalt mixtures with and without FRs, the fire simulation results in terms of the environmental conditions inside the tunnel are analyzed and compared with each other, also examining the safety of users involved in the fire. Then, the paper presents conclusions and discusses practical implications, along with suggestions for future studies.

2 Materials and Methodological Approach

2.1 Road Tunnel

The geometric dimensions of the road tunnel being examined are described in Fig. 1a,b. The input parameters related to traffic flow and ventilation conditions along it are given in Table 1, which also provides the properties of the materials used in the numerical simulation.

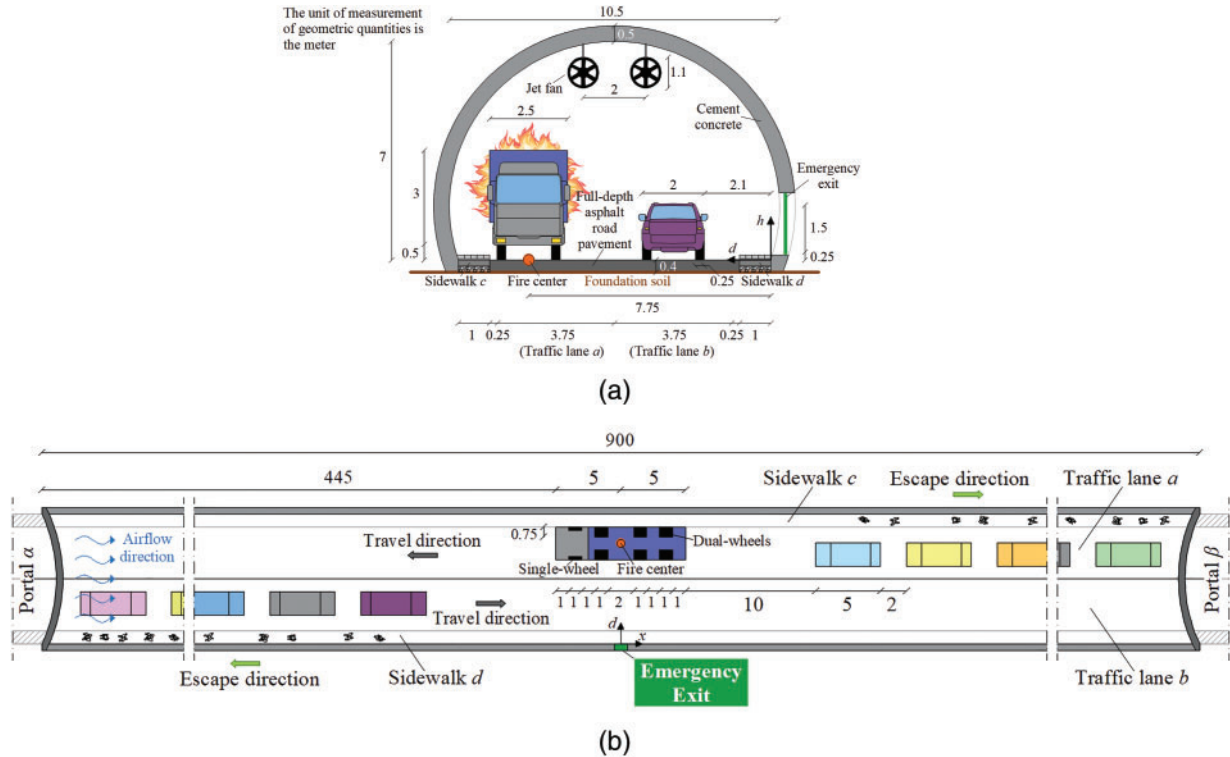


Figure 1: Road tunnel being investigated: (a) Transverse section; (b) Top view

Regarding the transverse section, the tunnel presents a horseshoe shape, which reaches up to 7 m in height and 10.5 m in width, for an area of 63 m². It includes two sidewalks, two shoulders, and two traffic lanes. The tunnel is rectilinear and level, with a length of 900 m and an emergency exit located midway. With the aim of making a more conservative analysis, the traffic flow (which is bi-directional) is assumed to be congested in both driving directions when the fire occurs. Regarding the materials used in the tunnel, cement concrete is used for the ceiling and walls, while three layers of dense-graded asphalt mixtures form the full-depth road pavement that lies directly on the foundation soil.

This tunnel is considered to be part of the Trans-European Road Network and, due to its length exceeding 500 m, falls under the regulations of European Directive 2004/54/EC [1]. According to this directive, mechanical ventilation systems are not mandatory for tunnels less than 1 km in length, as in the present study. Nevertheless, for making a comparison, the examined tunnel was assumed to be either naturally or mechanically ventilated. Regarding the case of natural ventilation, it is assumed to be generated by the movement of vehicles along the structure (i.e., the piston effect) and reproduced by applying a positive pressure difference ($+\Delta P$) between Portal α (i.e., the one downstream of the fire) and Portal β (i.e., the

one upstream of the burning source), both modeled as surfaces open to the external environment. In bi-directional road tunnels such as the one considered in the present study, this pressure difference tends to be significantly reduced or even neutralized due to the presence of opposing traffic flows. This is the reason why a $+\Delta P$ of only 0.5 Pa was applied [20]. When the tunnel is equipped with a longitudinal mechanical ventilation system, airflow within the structure—consistently directed toward Portal β —results from the combined effect of the previously mentioned piston effect and the operation of eight pairs of axial jet fans installed beneath the tunnel ceiling. These jet fans are programmed to activate automatically upon detection by the fire alarm system, which occurs after $t_{fire_alarm} = 100$ s from when the fire starts [21].

Table 1: The input parameters regarding traffic flow, material properties, and ventilation conditions

Input parameter	Value
<i>Traffic flow</i>	
Peak hourly volume [vehicles/h for each travel direction] [22]	1600
% of cars, % of heavy goods vehicles, and % of buses	75, 23, and 2
<i>Cement concrete</i> [23]	
Thickness [m]	0.5
Apparent density [kg/m^3]	2585
Thermal conductivity [$\text{W}/(\text{m}\cdot\text{K})$]	1.67
Specific heat [$\text{kJ}/(\text{kg}\cdot\text{K})$]	0.94
Emissivity coefficient [-]	0.9
<i>Dense-graded asphalt mixtures</i> [24]	
Thickness [m]	0.4
Apparent density [kg/m^3]	2275
Thermal conductivity [$\text{W}/(\text{m}\cdot\text{K})$]	0.563
Specific heat [$\text{kJ}/(\text{kg}\cdot\text{K})$]	0.88
Emissivity coefficient [-]	0.91
<i>Natural ventilation</i>	
Ambient pressure [Pa] [18]	101,325
$+\Delta P$ [Pa]	0.5
<i>Longitudinal mechanical ventilation</i>	
Longitudinal distance between Portal α and the first pair of jet fans [m]	115
Longitudinal distance between two consecutive pairs of jet fans [m]	90
Transverse space between each pair of jet fans [m]	2
Length of each jet fan [m]	2
Diameter of each jet fan [m]	1.1
Activation time (t_{fire_alarm}) of all the jet fans [s]	100
Maximum ventilation velocity of each jet fan [m/s]	25

2.2 Fire and Escape Scenarios

Table 2 shows the input parameters related to the geometric dimensions of the burning HGV, the value of the corresponding HRR_{max} and the time (t_{max}) required to reach it, as well as their heat of combustion and yields of fire products (i.e., soot and CO). Additionally, it also includes the geometric dimensions of the equivalent queuing cars and their wheels. Regarding this, the traffic flow—composed of 75% cars, 23% HGVs, and 2% buses—was converted into a queue of equivalent cars. Each equivalent car represents a vehicle whose dimensions were adjusted to account for the different sizes of cars, heavy goods vehicles, and buses in the queue. This approach simplifies the 3D CFD modeling by providing a uniform representation of the vehicle queuing upstream and downstream of the burning HGV.

Table 2: The input parameters regarding dimensions, maximum Heat Release Rate (HRR_{max}) and time (t_{max}) required to reach it, heat of combustion, and yields of combustion products (i.e., soot and CO) set for the HGV in flames and its wheels, as well as dimensions of the equivalent queued cars and their wheels

Vehicle	Dimensions [m]				HRR_{max} [MW]	t_{max} [min]	Heat of combustion [MJ/kg] [25]	Yields [kg/kg]	
	Length	Width	Height	Distance from road surface				Soot [26]	CO [26]
HGV in flames	10	2.5	3	0.5	100	10	25	0.025	0.15
Single-wheel	1	0.25	0.5	–					
Dual-wheels	1	0.75	0.5	–					
Equivalent queued car	5	2	1.5	0.25			Nonflammable		
Single-wheel	0.75	0.25	0.25	–					

The burning source, consisting of an HGV, is supposed to come into the tunnel via Portal β and catch fire near sidewalk c (Fig. 1a) after traveling 450 m in the tunnel (i.e., half its length). In the simulations, the HGV is modeled as a parallelepiped, as is each of its wheels, whose arrangement beneath the cargo and cabin is depicted in Fig. 1b. Concerning the HRR curve over time corresponding to the burning of both the HGV and its wheels, it features a linear growth phase until $t_{max} = 10$ min, followed by a steady phase that takes 5 min during which the fire power remains constant at the HRR_{max} of 100 MW. Each fire scenario was simulated over a 15-min duration, representing the period prior to the potential arrival of the firefighters. Fig. 2 depicts the HRR curve over time corresponding to the burning of both the HGV and its wheels.

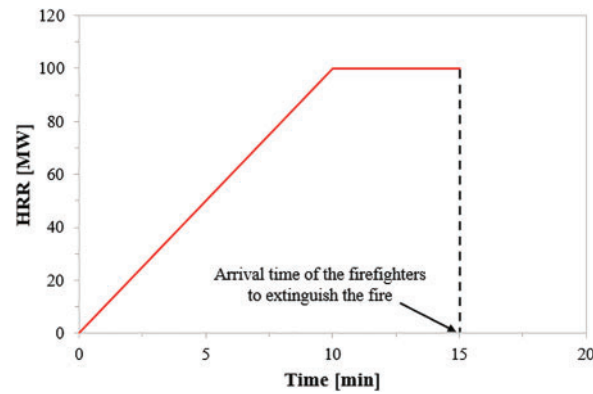


Figure 2: Heat Release Rate (HRR) curve over time corresponding to the burning of both the heavy goods vehicle and its wheels

Since the hypothesis of congested bi-directional traffic was considered, the tunnel is assumed to be fully occupied by stationary equivalent vehicles when the fire occurs. These equivalent cars are supposed not to overtake the HGV in flames, thus filling the whole traffic lane *a* upstream and the entire traffic lane *b* downstream of the fire. By assuming that the space between two successive equivalent queuing cars, and between the first equivalent queued car and the burning HGV is as shown in Fig. 1b (i.e., 2 and 10 m, respectively), the number of equivalent cars queuing in the tunnel was estimated to be equal to 62 for each travel direction. Assuming an average occupancy of 2.1 persons per equivalent queued vehicle [4], the fire might endanger the lives of 130 people for each travel direction. It is also worth noting that the generic equivalent queued car is schematized in the 3D CFD modeling as a nonflammable rectangular block, as is each of its four wheels. This was made to capture the impact due to the road pavement combustion alone when the HGV is in flames.

2.3 Road Pavement Combustion

In the 3D CFD modeling, the burning of the road pavement is replicated by means of the $T_{ignition}$ parameter, which identifies the temperature of the asphalt surface at which it could start to ignite because of its exposure to fire. Regarding the value of this parameter, there is no universally accepted reference in current literature. This is attributable to several factors, including the heat flux to which the asphalt surface is exposed, the quality and type of aggregates, the content of bitumen and voids in the asphalt mixture, the bitumen properties (e.g., softening point, penetration grade, etc.), as well as the type and amount of FRs added to traditional asphalt mixtures. Yang et al. [15], for example, found that an average value of $T_{ignition}$ for the flame-retarded asphalt materials is about 420°C. In contrast, a recent study [4] considered a $T_{ignition}$ of 250°C for the asphalt mixtures without FRs.

Once the road pavement consisting of asphalt mixtures with or without FRs has started the combustion process because its surface has reached the corresponding $T_{ignition}$ mentioned above, the asphalt pavement is assumed to contribute to the worsening of environmental conditions inside the tunnel in terms of HRR Per Unit Area (HRRPUA), as well as the release of soot, CO, and CO₂ expressed in terms of Mass Flow Rate Per Unit Area (MFRPUA), the average values of which measured experimentally by Xia et al. [5] were assumed in our numerical simulations. Table 3 shows the input parameters related to $T_{ignition}$, average HRRPUA, and average MFRPUA of soot, CO, and CO₂ set for both asphalt mixtures.

Table 3: The input parameters regarding ignition temperature (T_{ignition}), average HRR Per Unit Area (HRRPUA), and average Mass Flow Rate Per Unit Area (MFRPUA) of soot, CO, and CO₂ set for the asphalt mixtures containing or not Flame Retardants (FRs)

Asphalt mixtures	T_{ignition} [°C]	HRRPUA [kW/m ²]	MFRPUA $\times 10^{-4}$ [kg/(m ² ·s)]		
			Soot	CO	CO ₂
Without FRs	250	40.34	10.1	2.4	65.4
With FRs	420	32.51	7.6	0.1	40.2

It is also important to clarify that while the HRRPUA values are prescribed, the actual burning surface area of the road pavement is not. In the simulation, the ignition and subsequent combustion of the asphalt surface are triggered by thermal feedback from the fire (in this case, initiated by the burning HGV), and therefore the extent and timing of road pavement involvement emerge as part of the simulation outcome.

2.4 Research Framework

This work falls within the research field on improving the fire reaction of traditional asphalt mixtures for flexible pavements used in road tunnels. A 3D CFD modeling is developed and the use of flame-retarded asphalt mixtures, as opposed to conventional ones without FRs, is investigated. The paper might contribute to increasing the current state of knowledge by understanding how the FRs may mitigate the negative impacts on user safety and firefighters due to the combustion of the asphalt road pavement in the event of a large fire in a tunnel. This study may provide additional insights into research about the use of more fire-resistant asphalt pavements.

Fig. 3 shows a graphic representation of the methodological process followed.

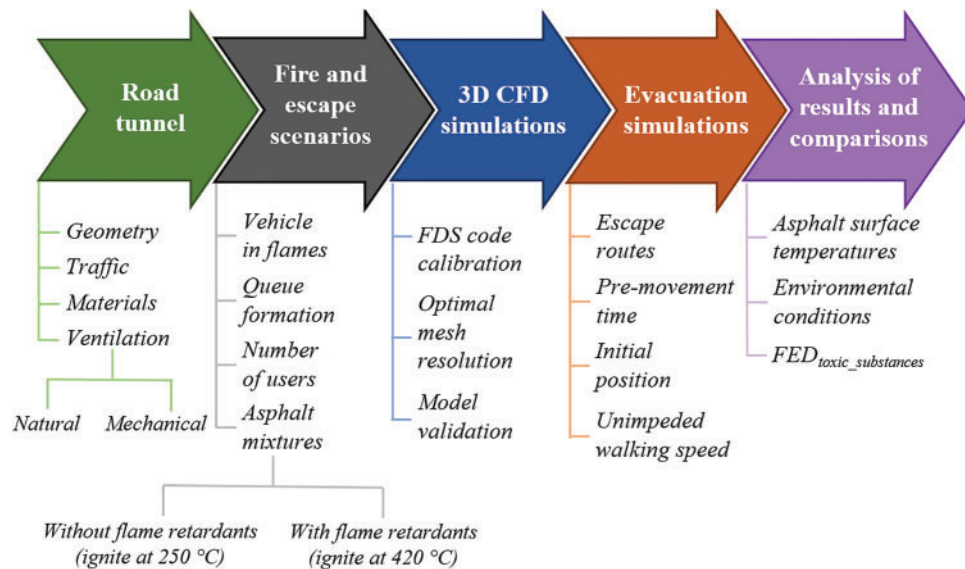


Figure 3: Graphic representation of the methodological process followed

3 3D CFD Simulations

3.1 Overview and Calibration of the Fire Dynamics Simulator (FDS) Code

Fire simulations were run using the FDS version 6.7.3 tool, an open-source 3D CFD code in which a simplified form of the Navier-Stokes equations is solved numerically [18].

FDS is one of the most frequently applied tools worldwide for simulating tunnel fire dynamics. Nevertheless, it was first calibrated against an experimental study conducted by Xue et al. [27] in a small-scale tunnel. A brief description of the configuration of this experimental test is given in Table 4, along with the combustion, turbulence, and thermal radiation models implemented in our FDS simulations to reproduce it.

Table 4: FDS tool calibration process: the configuration of the experimental test performed by Xue et al. [27] and the selected combustion, turbulence, and thermal radiation models set in our FDS simulations to reproduce it

Input parameter	Value
<i>Small-scale tunnel configuration [27]</i>	
Length [m]	6
Width [m]	0.9
Height [m]	0.3
Fuel type	Liquefied petroleum gas
Size of the fire pool [m ²]	0.18 × 0.15
HRR [kW]	3.15
Longitudinal ventilation flow [m/s]	0.13
<i>Models implemented in our FDS simulations [18]</i>	
Combustion	Mixing-controlled approach
Turbulence	Very large eddy simulation method
Thermal radiation	Solving the radiation transport equation for a gray gas

Given that the temperatures predicted by the FDS tool were found to be close to those experimentally measured by Xue et al. [27] (the error was below 5%), the same combustion, turbulence, and thermal radiation models listed in Table 4 were also used to set up the proposed 3D FDS modeling of the full-scale tunnel under examination.

3.2 Optimal Mesh Resolution

3.2.1 Subdivision of the Entire Calculation Domain

Within the FDS tool, the computational domain is divided into one or more 3D grids consisting of parallelepiped elements, preferably cubic for better numerical accuracy and stability. Each cell represents a control volume where the temperature, velocity, visibility distance, species concentration, and other physical quantities are estimated over time. Given that the precision of these estimates depends largely on the dimension of the 3D computational grids, the next step after calibrating the software was to define the optimal mesh size for the case examined. The optimal dimension δ_x [m] of a mesh element is usually sought in the range $D^*/16 \leq \delta_x \leq D^*/4$ [28], with the characteristic fire diameter D^* [m] equal to:

$$D^* = \left(\frac{Q}{\rho_\infty \times c_p \times T_\infty \times \sqrt{g}} \right)^{\frac{2}{5}} = \left(\frac{100,000}{1.204 \times 1.005 \times 293 \times \sqrt{9.81}} \right)^{\frac{2}{5}} = 6.1 \text{ m} \quad (1)$$

where Q is the HRR [kW], ρ_∞ is the density of air [kg/m³], c_p is the specific heat of air [J/(kg·K)], T_∞ is the ambient temperature [K], and g is the gravity acceleration [m/s²]. Then, the cell sizes to be included in the grid sensitivity analysis should be chosen in the range of 0.38–1.52 m, being $D^* = 6.1$ m for a 100 MW fire.

Considering the case where the road pavement is made of asphalt mixtures without FRs for a more conservative approach, Fig. 4 shows the influence of the cubic element size (i.e., 0.4, 0.5, 0.8, and 1 m) on the temperature predictions at Points 1, 2, and 3 at $t_{\max} = 10$ min after the fire onset in the case where the tunnel is mechanically and naturally ventilated. This figure also displays the d and h coordinates of each of these points, which are all taken 8 m upstream of the fire center. The location of Points 1, 2, and 3 ensures that the effects of the cubic cell size on the temperature predictions are analyzed over as wide a range of possible values as possible.

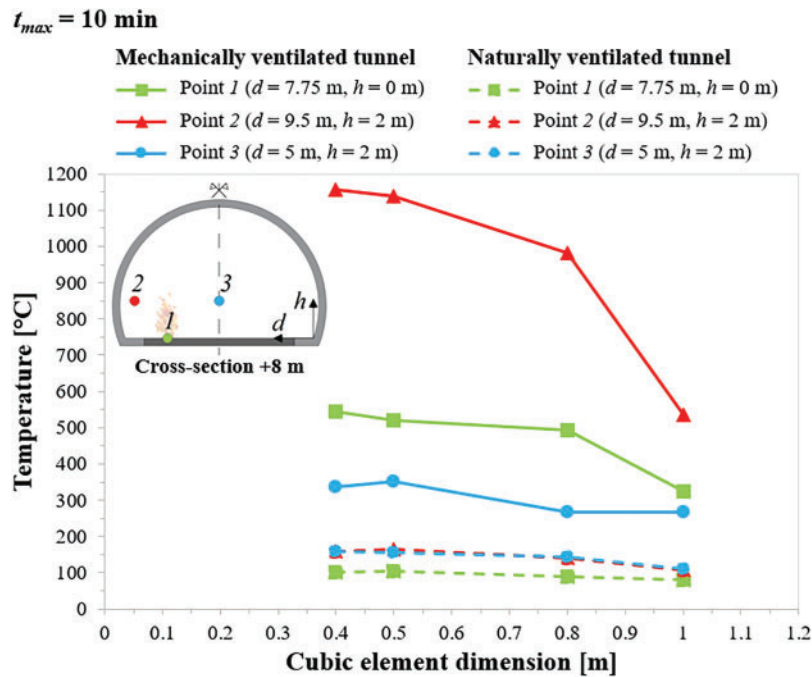


Figure 4: The influence of the cubic element dimension on the temperature predictions at Points 1, 2, and 3 at $t_{\max} = 10$ min following the onset of the fire in the case where the tunnel is mechanically and naturally ventilated

It is to be said that when the tunnel is mechanically ventilated, the airflow along the structure, induced by the activation of jet fans, was found to be stronger than in the case of natural ventilation. This promotes a more effective upstream transport of hot gases generated by the fire. Therefore, since all measurement points are located upstream of the burning vehicle, the temperature at Points 1, 2, and 3 in the mechanically ventilated tunnel is expected to be higher than that observed under natural ventilation conditions.

As shown in Fig. 4, a grid dimension of 0.5 m side is fine enough for the problem under examination, providing that the temperatures do not differ more than 5% from those obtained using the finest mesh (i.e., 0.4 m). Consequently, the entire computational domain is discretized into cubic elements with a side length of 0.5 m.

3.2.2 Discretization of the Tunnel Region Where the Asphalt Pavement Is Most Likely to Burn

With the aim of better capturing the contribution of road pavement burning in the event of a tunnel fire, a refined 3D mesh with cubic cells of 0.25 m side (i.e., half of the 0.5 m mesh size defined above) is adopted to subdivide the computational domain where the asphalt surface is most likely to burn since its temperature is $\geq T_{\text{ignition}}$.

With reference to asphalt mixtures without FRs (i.e., $T_{\text{ignition}} = 250^\circ\text{C}$), Fig. 5a,b shows the tunnel length where the asphalt surface temperatures are $\geq T_{\text{ignition}} = 250^\circ\text{C}$ at $t = 15$ min since the HGV ignition when the tunnel is mechanically and naturally ventilated, respectively.

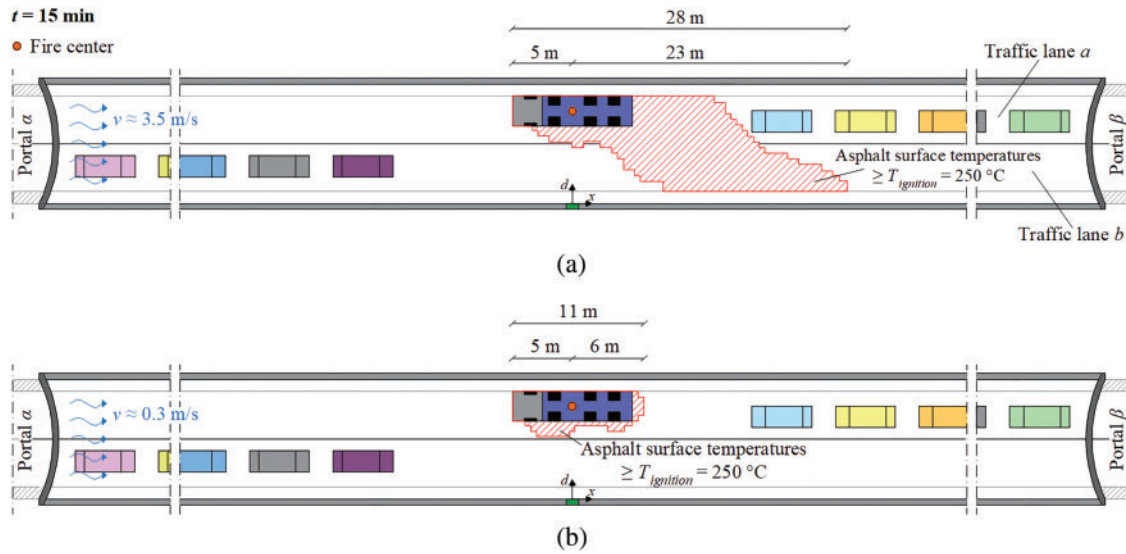


Figure 5: Determination of the tunnel length where the asphalt surface temperatures are $\geq T_{\text{ignition}} = 250^\circ\text{C}$ at $t = 15$ min after the fire onset in the case where the tunnel is: (a) mechanically ventilated; (b) naturally ventilated

Comparing these two figures, it can be seen that the tunnel region where the asphalt surface might burn is much longer when the tunnel is mechanically rather than naturally ventilated (i.e., 28 m vs. 11 m), with a larger difference found upstream of the fire center (i.e., 23 m against 6 m). This is because the hot gases caused by the fire (i.e., from both the HGV and the road pavement) are pushed further towards Portal β under longitudinal mechanical ventilation conditions, where the airflow along the tunnel has an average velocity (v) of approximately 3.5 m/s, compared to around 0.3 m/s in the scenario of natural ventilation.

Fig. 5a also shows how the asphalt surface temperatures $\geq T_{\text{ignition}} = 250^\circ\text{C}$ extend upstream of the fire center for a longer distance along the traffic lane b. This might be caused by the equivalent queued vehicles, which tend to hinder the spread of the hot gases generated by the fire along the traffic lane a, diverting them to the adjacent traffic lane b free of obstacles.

Fig. 6a,b shows the optimal mesh resolution identified when the tunnel is mechanically and naturally ventilated, respectively. Compared with the previously defined longitudinal extent, the length of the tunnel region where the asphalt surface is most likely to burn because its temperature is $\geq T_{\text{ignition}} = 250^\circ\text{C}$ is increased by 1 m in both directions to adopt a more conservative approach. This results in a total length of 30 m under longitudinal mechanical ventilation conditions—comprising 24 m upstream and 6 m downstream from the HGV center (Fig. 6a)—and 13 m in the case of natural ventilation—with 7 m upstream and 6 m downstream from the fire center (Fig. 6b).

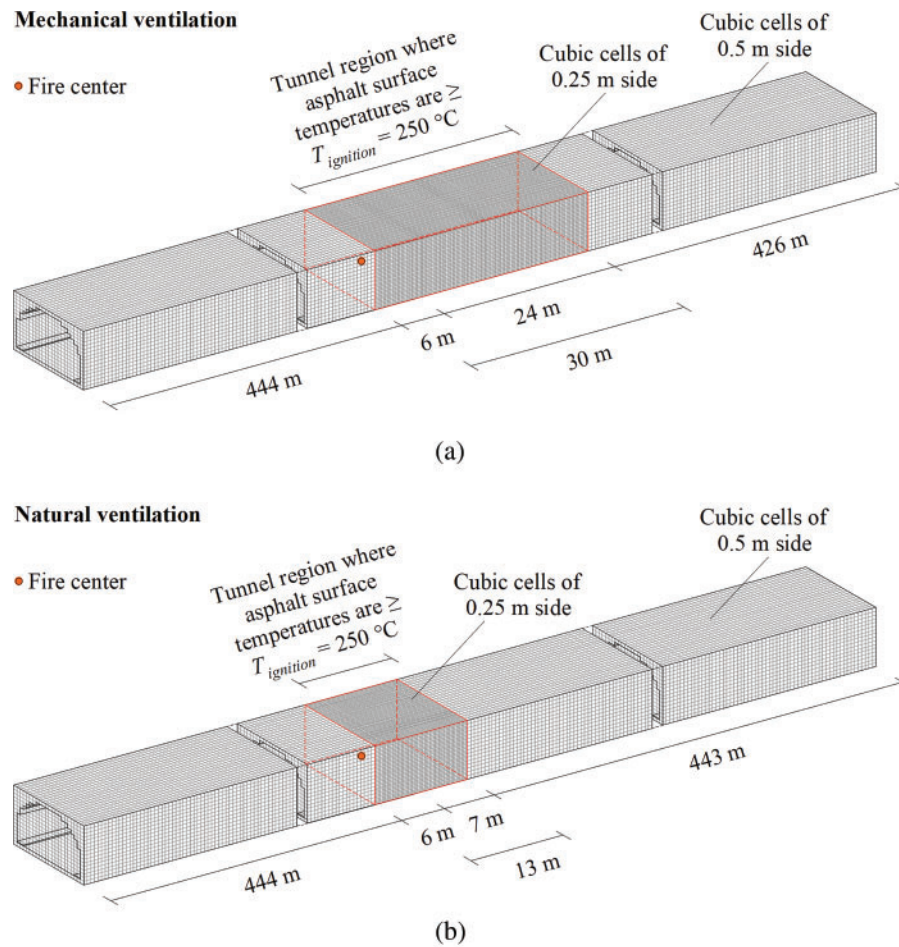


Figure 6: Optimal mesh resolution in the case where the tunnel is: (a) mechanically ventilated; (b) naturally ventilated

Therefore, the proposed 3D FDS modeling is composed of a total of 826,496 cubic cells under longitudinal mechanical ventilation conditions, while it is made up of a total of 757,504 cubic elements when the tunnel is naturally ventilated.

3.3 Model Validation

In order to validate the proposed 3D FDS modeling, it was thought to replicate the study by Avenel et al. [29] involving a fire characterized by a thermal power of 30 MW in a naturally ventilated road tunnel affected by bi-directional traffic. Fig. 7 compares the changes over time of the asphalt surface temperature at the fire center predicted by the developed 3D FDS model with those reported by Avenel et al. [29]. It is worth noting that the two temperature profiles show close agreement, with differences of no more than 5% in the times required to reach the T_{ignition} of 250°C for asphalt mixtures without FRs and 420°C for asphalt mixtures with FRs.

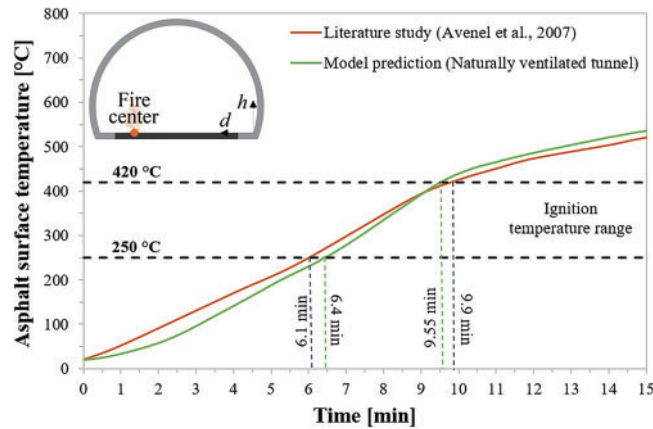


Figure 7: Comparison of the temporal evolution of the asphalt surface temperature at the fire center provided by the proposed 3D FDS modeling with that obtained by Avenel et al. [29]

Considering this, the authors are convinced that their 3D FDS modeling was configured properly for both asphalt mixtures.

It is to be stressed that among the approaches for validating the FDS model presented in our paper, we decided to compare the results obtained with those of the reduced-scale tunnel fire experiment (100 m-long) reported in the mentioned study by Avenel et al. [29]. The use of a small-scale experiment was necessary due to both the lack of full-scale experiments in literature regarding the contribution of asphalt pavement burning during a tunnel fire, and the technical and economic difficulties of conducting a real-scale experiment, the results of which would, in any case, be affected by uncertainties.

4 Evacuation Simulations

The FDS code includes an egress module called Evac [19], which was applied to simulate the process by which people leave the structure when the fire occurs. It enables parameters such as unimpeded walking speed (v_0), pre-movement time, initial location inside the tunnel, evacuation route, and tunnel exit to be assigned to the individual person or a group of users, who are considered to move in a 2D horizontal space. The value attributed to each of these parameters is reported in Table 5.

Table 5: The input parameters regarding unimpeded walking speed, pre-movement time, initial location within the tunnel, escape route, and tunnel exit of each user set in the Evac code

Input parameter	Value
Unimpeded walking speed of each user [m/s]	0.3
Pre-movement time of each user [s] [4]	130
Initial location along the tunnel of each user	Adjacent to the corresponding equivalent car
Evacuation route (Fig. 1b)	Sidewalk d and sidewalk c for people downstream and upstream of the HGV on fire, respectively
Tunnel exit (Fig. 1b)	Portal α and Portal β for users downstream and upstream of the fire, respectively*

Note: *Users are unable to reach the emergency exit since it is situated near the fire at the midpoint of the tunnel length.

For each agent, according to Eq. (2) [19], the Evac code calculates the cumulative (i.e., considering their entire escape process towards a safe place) Fractional Effective Dose (FED) due to the inhalation of toxic substances like CO and CO₂ (FED_{toxic_substances}), the levels of which over time are imported by the FDS code:

$$\text{FED}_{\text{toxic_substances}} = (\text{FED}_{\text{CO}} + \text{FED}_{\text{CN}} + \text{FED}_{\text{NO}_x} + \text{FLD}_{\text{irr}}) \times \text{HV}_{\text{CO}_2} + \text{FED}_{\text{O}_2} \quad (2)$$

where FED_{CO} accounts for the fraction of the incapacitating dose of carbon monoxide, FED_{CN} represents the contribution of cyanide, FED_{NO_x} refers to nitrogen oxides exposure, FLD_{irr} quantifies the effect of respiratory irritants, HV_{CO₂} is the hyperventilation factor induced by carbon dioxide, and FED_{O₂} considers the hypoxic effects due to reduced oxygen concentration. Hence, the number of potential casualties in a certain fire scenario is given by the sum of the users who have a FED_{toxic_substances} above a threshold value, which denotes the point at which the agent would no longer be able to self-evacuate the tunnel. In our case, this threshold value was assumed to be 0.3 [30].

The rate of entry of equivalent cars into the tunnel was estimated to be one every 2.25 s. This implies that at $t_{\text{fire_alarm}} = 100$ s after the fire onset (i.e., at the time the fire alarm system is triggered), there are only 44 equivalent vehicles (i.e., 92 people) queued for each travel direction. In order to consider that the 38 occupants of the remaining 18 equivalent cars in the queue for each travel direction will enter the structure over the following approximately 40 s, an extra-premovement time—corresponding to the delay between the fire alarm system being triggered and the moment these individuals actually enter the tunnel—is assigned to each of them.

5 Examination and Discussion of the Findings

5.1 Surface Temperature Distribution of the Road Pavement

5.1.1 Non-Flame-Retarded Asphalt Mixtures

Fig. 8a,b illustrates the surface temperature distribution of the non-flame-retarded asphalt pavement around the fire at $t = 2, 10$, and 15 min since the HGV ignition in the case where the tunnel is mechanically and naturally ventilated, respectively.

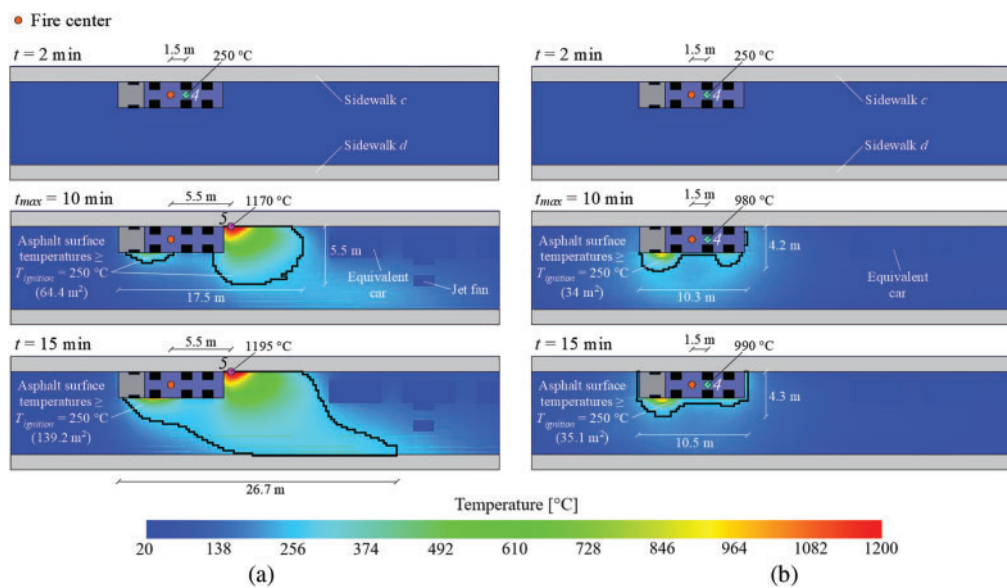


Figure 8: Surface temperature distribution of the non-flame-retarded asphalt pavement around the fire at 2, 10, and 15 min after its onset in the case where the tunnel is: (a) mechanically ventilated; (b) naturally ventilated

Considering both cases of longitudinal mechanical and natural ventilation, the asphalt surface was found to start burning at Point 4, where the T_{ignition} of 250°C is reached about 2 min after the fire onset. As can be seen from Fig. 8a,b, this point is located in the middle of the burning vehicle's four wheels forming its rear axle closest to the fire center (i.e., 1.5 m upstream of it). Obviously, the combustion of these wheels contributed to a more rapid rise in the asphalt surface temperatures in the region surrounding them. It is also to be said that the road pavement began to ignite slightly upstream of the HGV in flames since both the longitudinal mechanical and natural ventilation tend to drive the hot gases generated by the fire in the direction of Portal β . Given that the average velocity of the airflow along the structure is still comparable in both ventilation scenarios adopted at $t = 2$ min (all the jet fans were supposed to activate about 1.7 min after the HGV ignites), the road pavement started to burn at the same Point 4 regardless of whether the tunnel is mechanically or naturally ventilated.

Fig. 8a,b also reveals that the asphalt surface temperature increases from $t = 2$ min to $t = 15$ min in both ventilation conditions examined. This results from the gradual increase in the intensity of the burning vehicle over time, the extinguishment of which by the firefighters is assumed to begin only 15 min after the start of the fire. However, at $t_{\text{max}} = 10$ min and $t = 15$ min, substantial differences in the values and distributions of road pavement temperatures can be noted between the cases of longitudinal mechanical and natural ventilation. This is due to the fact that the airflow along the tunnel under the condition of longitudinal mechanical ventilation, having now achieved the average velocity of 3.5 m/s, pushes the hot gases more towards Portal β and, as a result, also a larger area of the asphalt surface that could ignite is observed.

Discussing the case of longitudinal mechanical ventilation in detail (Fig. 8a), it can be seen that 10 min after the fire onset, the area of the burning road pavement is about 64 m^2 , as well as the maximum temperature of the asphalt surface is equal to around 1170°C and is found at Point 5. At $t = 15$ min, the area of the road surface that could ignite has increased (i.e., nearly 139 m^2), and the maximum temperature of the asphalt surface at Point 5 is approximately 1195°C .

When the tunnel is naturally ventilated, Fig. 8b reveals that at $t_{\text{max}} = 10$ min, the area of the asphalt surface susceptible to ignition is smaller (i.e., around 34 m^2), and the maximum temperature of the asphalt surface is equal to about 980°C and is observed at Point 4. At $t = 15$ min, there is a slight increase in the extent of the area of the burning road pavement (i.e., about 35 m^2), and the maximum temperature of the asphalt surface of about 990°C is still found at Point 4.

5.1.2 Flame-Retarded Asphalt Mixtures

Fig. 9a,b displays the surface temperature distribution of the asphalt pavement with FRs surrounding the fire at $t = 3, 10$, and 15 min since the HGV ignition under longitudinal mechanical and natural ventilation conditions, respectively.

From Fig. 9a,b, it can be noted that: (i) in both ventilation scenarios examined, the asphalt surface starts burning at Point 4, where the T_{ignition} of 420°C is reached at $t \approx 3$ min; (ii) the extent of the road surface reaching temperatures $\geq T_{\text{ignition}} = 420^{\circ}\text{C}$ expands over time; (iii) under longitudinal mechanical ventilation conditions, the area of the burning asphalt surface is about 44 m^2 at $t_{\text{max}} = 10$ min and around 58 m^2 at $t = 15$ min, and the maximum temperature of the road pavement at Point 5 is approximately 1100°C and 1120°C , respectively; (iv) under natural ventilation conditions, the extent of the road surface reaching temperatures $\geq T_{\text{ignition}} = 420^{\circ}\text{C}$ is about 28 m^2 at $t_{\text{max}} = 10$ min and around 31 m^2 at $t = 15$ min, and the maximum temperature of the road surface at Point 4 is approximately 886°C and 892°C , respectively.

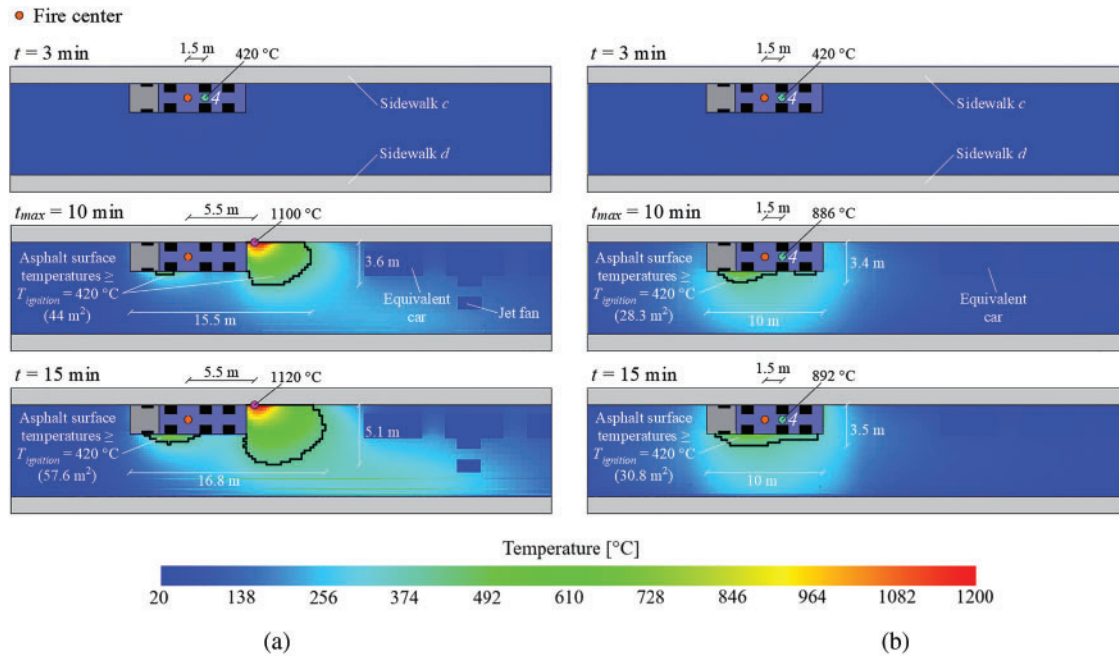


Figure 9: Surface temperature distribution of the flame-retarded asphalt pavement around the fire at 3, 10, and 15 min after its onset in the case where the tunnel is: (a) mechanically ventilated; (b) naturally ventilated

Comparing Fig. 9a with Fig. 8a, as well as Fig. 9b with Fig. 8b, it can be seen that the use of flame-retarded asphalt mixtures, as opposed to traditional ones without FRs, leads to: (i) an increase in the ignition time of the road pavement by about 1 min; (ii) a significant reduction in the extension of the area of the asphalt surface that might burn; (iii) a decrease in the peak temperature reached by the road surface.

5.2 Tunnel Environmental Conditions at $t_{\max} = 10$ min to Analyze the Safety of Occupants

Since the airflow along the structure was assumed to move from Portal α to Portal β , the environmental conditions inside the tunnel during the fire could especially threaten the safety of users situated upstream of the HGV in flames. This is because fire products, such as hot gases and toxic substances, are carried in the same direction as their evacuation. With the aim of evaluating the capacity of users to self-evacuate the structure during the 100 MW fire being examined, this section shows the environmental conditions upstream of the fire at $t_{\max} = 10$ min after its onset when the tunnel is mechanically (violet lines) and naturally (green lines) ventilated, considering both cases of the road pavement made of asphalt mixtures with (dotted lines) and without (continuous lines) FRs. The longitudinal profiles describing the concentration levels of CO and CO₂, as well as FED_{toxic_substances}, for the aforementioned Point 2 (i.e., situated upstream of the fire center at the human breathing height of 1.85 m above the sidewalk c, which represents the escape route for people fleeing towards Portal β) are given below. The longitudinal profiles also show the corresponding threshold value for human health, along with the distance traveled upstream of the fire center by the last person leaving the tunnel via Portal β (i.e., the one in the first equivalent queued car upstream of the burning vehicle). This distance was estimated based on the average actual walking speed and assuming that the mentioned user is initially situated approximately 15 m upstream of the fire center. The 15 m result from the sum of half the HGV's length (i.e., 5 m) and the space between the burning vehicle and the first equivalent car in the queue (i.e., 10 m) (Fig. 1b).

Taking into account both types of asphalt mixture, Table 6 shows the average actual walking speed and the distance (in brackets) from the HGV center of the last user exiting the structure through Portal β at $t_{\max} = 10$ min after the fire onset in the case where the tunnel is mechanically and naturally ventilated. It is worth noting that the average actual walking speed of the mentioned person, as well as their distance upstream of the burning vehicle center, decreases with increasing levels of toxic substances they are subjected to while leaving the structure. Exposure to higher concentration levels of CO and CO₂ arises when non-flame-retarded asphalt mixtures are employed in the tunnel.

Table 6: Average actual walking speed and distance (in brackets) from the fire center of the last user exiting the structure via Portal β at $t_{\max} = 10$ min after the fire onset when the tunnel is mechanically and naturally ventilated, for both cases of asphalt mixtures containing or not Flame Retardants (FRs)

Asphalt mixtures	Mechanically ventilated tunnel	Naturally ventilated tunnel
Average actual walking speed [m/s] and distance [m] (in Brackets) from the fire center of the last person exiting the tunnel through portal β at $t_{\max} = 10$ min after the fire onset		
Without FRs	0.0915 (58)	0.1660 (93)
With FRs	0.0936 (59)	0.1745 (97)

5.2.1 Concentration Levels of Toxic Substances

The use of flame-retarded asphalt mixtures, as opposed to conventional ones without FRs, was found to reduce the CO concentration levels both when the tunnel is mechanically (Fig. 10a) and naturally (Fig. 10b) ventilated. This reduction is remarkable up to a distance from the fire center of about 175 m and 120 m under longitudinal mechanical and natural ventilation conditions, respectively.

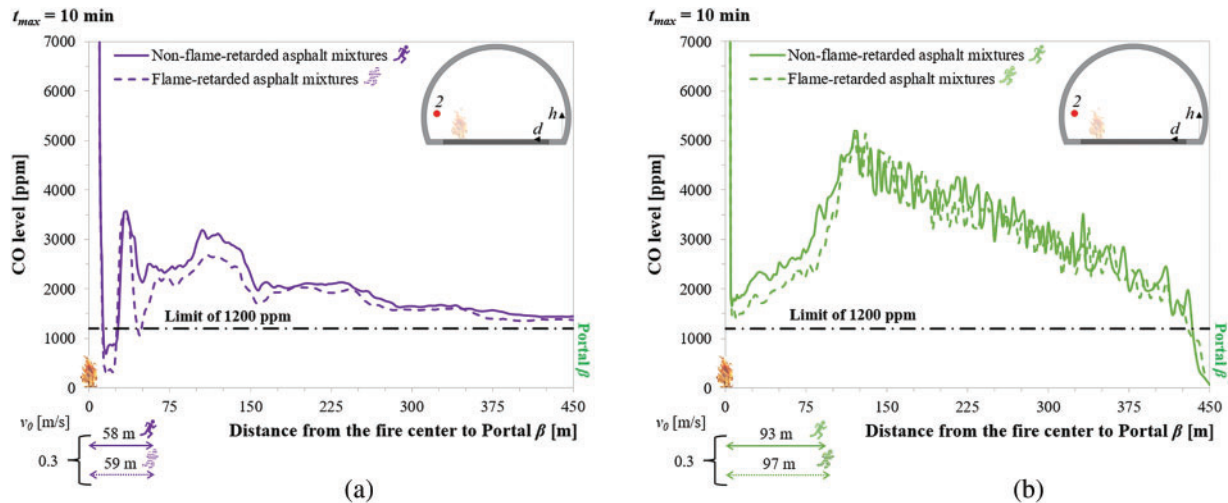


Figure 10: Longitudinal profiles describing the CO concentration level upstream of the fire at $t_{\max} = 10$ min after its onset for Point 2 when the road pavement consists of asphalt mixtures modified or not using flame retardants and the tunnel is: (a) mechanically ventilated; (b) naturally ventilated

Examining in detail Fig. 10a,b, it is also possible to note that the CO concentration, however, exceeds the corresponding threshold value for human health equal to 1200 ppm [31] along almost the entire tunnel portion between the fire center and Portal β , regardless of the type of asphalt mixture considered. This means that the CO level generated by the burning vehicle compared to that of road pavement is prevalent.

The use of flame-retarded asphalt mixtures, as opposed to conventional ones without FRs, was also found to reduce the CO₂ concentration both in the case where the tunnel is mechanically (Fig. 11a) and naturally (Fig. 11b) ventilated. In addition, Fig. 11a reveals that the CO₂ level remains below its critical limit for human safety of 40,000 ppm [31] upstream of the HGV in flames when a longitudinal mechanical ventilation system is present, with the sole exception of the immediate vicinity of the fire. In contrast, under natural ventilation conditions (Fig. 11b), the CO₂ concentration is above 40,000 ppm within a tunnel region from 92 to 235 m upstream of the fire center for non-flame-retarded asphalt mixtures, and between 107 and 197 m for flame-retarded asphalt mixtures. This means that the use of FRs reduces the longitudinal extension of the tunnel region where the CO₂ concentration exceeds the unacceptable limit for human safety under natural ventilation conditions.

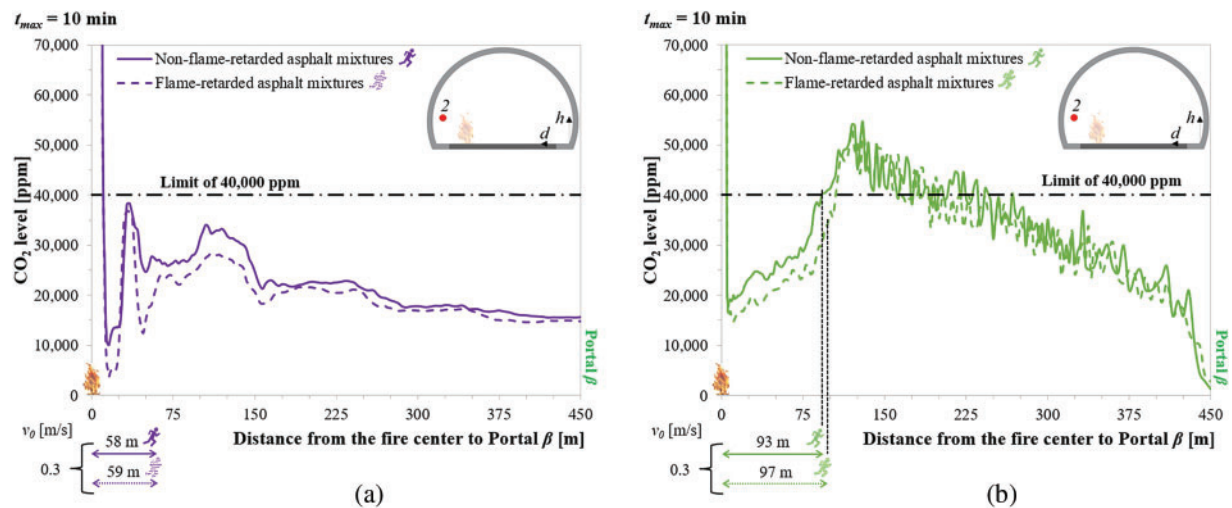


Figure 11: Longitudinal profiles describing the CO₂ concentration level upstream of the fire at $t_{\max} = 10$ min after its onset for Point 2 when the road pavement consists of asphalt mixtures modified or not using flame retardants and the tunnel is: (a) mechanically ventilated; (b) naturally ventilated

5.2.2 $FED_{\text{toxic_substances}}$

The effects of adding the FRs to asphalt mixtures were observed mainly in terms of the reduction in the CO and CO₂ levels, while almost negligible impacts were found in terms of the temperature, radiant flux, and visibility distance along the above-mentioned Point 2 of Figs. 10 and 11. The corresponding spatial profiles are therefore not reported in the present paper to save space.

A parameter that simultaneously considers both the CO and CO₂ concentration levels was subsequently used in our study. It is known in literature as $FED_{\text{toxic_substances}}$.

Fig. 12a,b shows that the values of $FED_{\text{toxic_substances}}$ upstream of the HGV in flames due to the combustion of flame-retarded asphalt mixtures being lower than those associated with the burning of asphalt mixtures without FRs, regardless of whether the tunnel is mechanically or naturally ventilated. However,

apart from in the region occupied by the vehicle in flames, the $FED_{\text{toxic_substances}}$ exceeds the tenable limit for human health, which was assumed to be equal to 0.3 [30], up to about 350 m from the fire center.

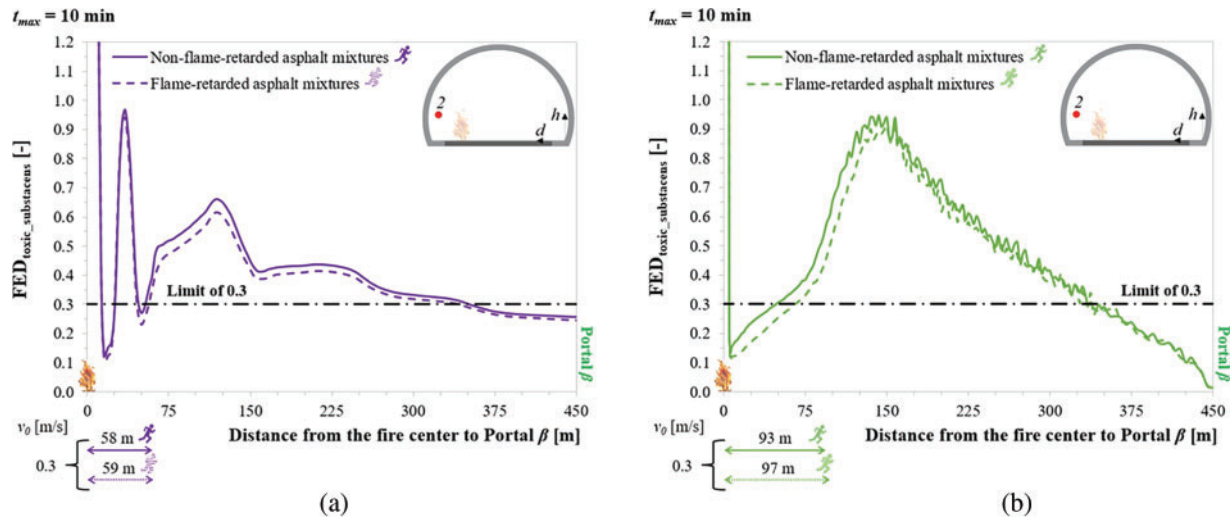


Figure 12: Longitudinal profiles describing the $FED_{\text{toxic_substances}}$ upstream of the fire at $t_{\text{max}} = 10$ min after its onset for Point 2 when the road pavement consists of asphalt mixtures modified or not using flame retardants and the tunnel is: (a) mechanically ventilated; (b) naturally ventilated

5.2.3 Number of Potential Victims

In each fire scenario examined, the number of potential casualties upstream of the burning source upon the arrival of firefighters at $t = 15$ min after the fire onset is estimated by counting how many users have a cumulative $FED_{\text{toxic_substances}}$ (i.e., considering their entire evacuation process up to Portal β) exceeding 0.3.

The use of flame-retarded asphalt mixtures, as opposed to conventional ones without FRs, resulted in fewer potential casualties upstream of the fire in both ventilation scenarios examined. However, this reduction is more evident under longitudinal mechanical ventilation conditions. The use of FRs into asphalt mixtures might allow 120 occupants to self-evacuate the structure through Portal β against 117 related to the case of non-flame-retarded asphalt mixtures under longitudinal mechanical ventilation conditions, as well 94 evacuees against 92 when the tunnel is naturally ventilated.

In this context, even marginal improvements in environmental conditions can provide evacuees with valuable additional time for escape, as well as allow firefighters to operate under more favorable and less hazardous circumstances. Furthermore, although the reduction in the number of casualties is limited, the improved conditions resulting from the use of flame-retarded asphalt mixtures could significantly benefit the health of survivors, who would likely experience lower exposure to toxic gases and thus less severe health effects. It is also worth noting that the implementation of flame-retarded asphalt mixtures might be relatively straightforward compared to other fire safety measures, such as the installation of active suppression (e.g., sprinklers) or ventilation systems, if not present.

5.3 Tunnel Environmental Conditions at $t = 15$ min to Study the Safety of Firefighters

Firefighters are expected to enter the tunnel using Portal α at $t = 15$ min to extinguish flames. By doing so, they will move through the structure in the same direction as the forced or natural airflow, thus benefiting from more favorable environmental conditions.

In order to determine the possible impact of FRs application on firefighters' ability to operate, this section describes the longitudinal profiles of CO (Fig. 13) and CO₂ (Fig. 14) levels downstream (i.e., for Point 6, which has the same d and h coordinates as Point 2 but is located downstream of the burning source) of the fire at $t = 15$ min after its onset in both cases of road pavement made of asphalt mixtures with and without FRs. Specifically, these longitudinal profiles are shown only for the scenario of natural ventilation (in the case of longitudinal mechanical ventilation and when the black-layering phenomenon is avoided as in our case, the tunnel portion downstream of the fire is free of smoke).

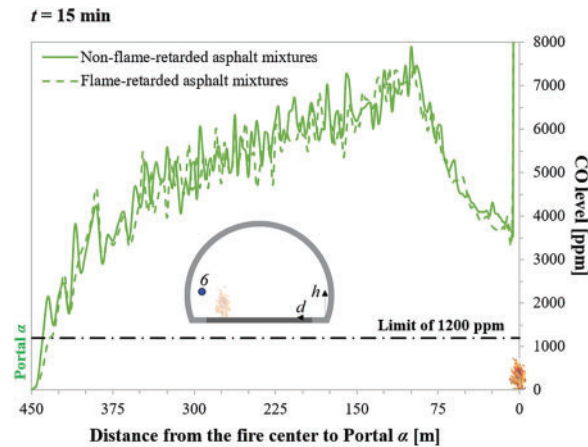


Figure 13: Longitudinal profiles describing the CO level downstream of the fire at $t = 15$ min after its onset for Point 6 when the road pavement consists of asphalt mixtures modified or not using flame retardants and the tunnel is naturally ventilated

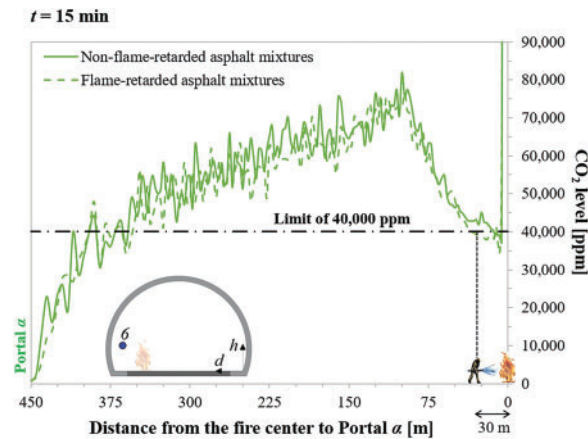


Figure 14: Longitudinal profiles describing the CO₂ level downstream of the fire at $t = 15$ min after its onset for Point 6 when the road pavement consists of asphalt mixtures modified or not using flame retardants and the tunnel is naturally ventilated

The use of flame-retarded asphalt mixtures, as opposed to conventional ones without FRs, was found to slightly reduce the CO (Fig. 13) and CO₂ (Fig. 14) levels. Consequently, an improvement in the environmental conditions for the operational effectiveness of the firefighting personnel downstream of the HGV in flames might be found (i.e., the curves of CO and CO₂ concentrations in the case of FRs lie almost always under

those associated with the asphalt mixtures without FRs). However, the CO and CO₂ levels exceed the corresponding tenability limits (i.e., 1200 ppm and 40,000 ppm, respectively) along an almost comparable tunnel portion downstream of the burning HGV, regardless of the type of road pavement adopted. This confirms that the smoke concentration produced by the HGV on fire compared to that of asphalt pavement is prevalent.

5.4 Considerations for Future Research

It is important to acknowledge that, as in any modeling-based study, this paper relies on a set of assumptions to keep the analysis practical and to focus on the core phenomena under examination. Particularly, even though these results are promising, more studies are needed to better understand the thermal properties (such as specific heat and thermal conductivity) and combustion parameters (like ignition temperature, heat release, and toxic emissions) of asphalt mixtures with flame retardants. Within this framework, to strengthen the understanding and validation of pavement-related fire dynamics, future research should include large-scale experimental investigations dedicated to asphalt pavement burning, as well as the use of cement concrete in road pavements used for tunnels. Furthermore, to fully assess the overall effectiveness and feasibility of adopting flame-retarded asphalt mixtures, future studies should also consider a broader range of potential fire scenarios and FR compositions, followed by a comprehensive cost–benefit analysis. The next investigation should focus on the above issues in order to further develop research.

Despite this need for additional studies, the developed 3D CFD modeling provides a realistic and scientifically rigorous framework for assessing the impact of asphalt pavement combustion on user safety during tunnel fires. Moreover, it retains general validity, and its results can be cautiously extended to other contexts with similar tunnel geometries, traffic characteristics, asphalt mixtures and FR compositions, ventilation conditions, and fire scenarios.

6 Conclusions

This article was primarily carried out to quantitatively assess whether the use of flame-retarded asphalt mixtures, as opposed to traditional ones without FRs, might contribute to lessening the negative impacts on the safety of occupants and the operability of firefighters caused by road pavement burning during a severe tunnel fire.

The analyzed road tunnel, measuring 900 m in length, experiences bi-directional traffic and operates under either longitudinal mechanical or natural ventilation. The burning vehicle, consisting of an HGV located at the midpoint of the tunnel length, was considered to develop a HRR_{max} of 100 MW within 10 min from its ignition. The road pavement was assumed to start burning when its surface temperature achieved 250°C in the case of non-flame-retarded asphalt mixtures and 420°C when the flame-retarded asphalt mixtures were used. Once ignited, the use of the FRs was investigated to understand if it contributed to a reduction of smoke in terms of the CO and CO₂ concentrations.

The proposed goals were pursued by developing 3D CFD modeling and solved using the FDS code, while the corresponding escape process of the users from the structure is reproduced by means of the Evac tool.

By using flame-retarded asphalt mixtures the following results were found: (i) a delayed ignition time of the asphalt pavement by around 1 min; (ii) a considerable reduction in the extension of the area of pavement surface that might burn; (iii) a reduction in the maximum temperature of the asphalt surface that might be achieved in the event of the aforementioned large fire; (iv) a reduction in CO and CO₂ concentration levels at the human breathing height along the escape route and, consequently, a decrease in $FED_{toxic_substances}$ values; (v) a minor number of tunnel occupants exposed to the risk of incapacity to self-evacuate; (vi) minor CO

and CO₂ concentration levels for the firefighters entering the tunnel downstream of the fire under natural ventilation conditions.

Future studies should explore asphalt thermal and combustion properties, conduct large-scale fire experiments, assess various FR compositions and fire scenarios, and perform cost–benefit analyses to evaluate the effectiveness and feasibility of adopting flame-retarded asphalt mixtures in road tunnels.

Acknowledgement: Not applicable.

Funding Statement: The authors received no specific funding for this study.

Author Contributions: The authors confirm contribution to the paper as follows: Conceptualization, Ciro Caliendo, Isidoro Russo and Gianluca Genovese; methodology, Ciro Caliendo, Isidoro Russo and Gianluca Genovese; software, Ciro Caliendo, Isidoro Russo and Gianluca Genovese; validation, Ciro Caliendo, Isidoro Russo and Gianluca Genovese; formal analysis, Ciro Caliendo, Isidoro Russo and Gianluca Genovese; investigation, Ciro Caliendo, Isidoro Russo and Gianluca Genovese; data curation, Ciro Caliendo, Isidoro Russo and Gianluca Genovese; writing—original draft preparation, Ciro Caliendo, Isidoro Russo and Gianluca Genovese; writing—review and editing, Ciro Caliendo, Isidoro Russo and Gianluca Genovese; visualization, Ciro Caliendo, Isidoro Russo and Gianluca Genovese; supervision, Ciro Caliendo. All the authors reviewed the results and approved the final version of the manuscript.

Availability of Data and Materials: The data that support the findings of this study are available from the Corresponding Author, Isidoro Russo, upon reasonable request.

Ethics Approval: Not applicable.

Conflicts of Interest: The authors declare no conflicts of interest to report regarding the present study.

Nomenclature

CFD	Computational fluid dynamics
CO	Carbon monoxide
FDS	Fire dynamics simulator
FR	Flame retardant
g	Gravity acceleration
HGV	Heavy goods vehicle
HRRPUA	Heat release rate per unit area
MFRPUA	Mass flow rate per unit area
Q	Heat release rate
t	Time elapsed since the fire onset
v	Average airflow velocity
c_p	Specific heat of air
CO ₂	Carbon dioxide
FED _{CN}	Fraction of the incapacitating dose of cyanide
FED _{CO}	Fraction of the incapacitating dose of carbon monoxide
FED _{NOx}	Fraction of the incapacitating dose of nitrogen oxides
FED _{O₂}	Fraction of the incapacitating dose of oxygen
FED _{toxic_substances}	Fractional effective dose due to the inhalation of toxic substances
HV _{CO₂}	Hyperventilation factor induced by carbon dioxide
HRR _{max}	Maximum heat release rate
t_{fire_alarm}	Activation time of all jet fans
$T_{ignition}$	Ignition temperature of the asphalt road surface
t_{max}	Time to reach the maximum heat release rate

T_{∞}	Ambient temperature
v_0	Unimpeded walking speed
$+\Delta P$	Positive pressure difference between the tunnel portals
ρ_{∞}	Density of air

References

1. European Parliament and Council. Directive 2004/54/EC on minimum safety requirements for tunnels in the Trans-European Road Network [Internet]. [cited 2025 Apr 18]. Available from: <https://eur-lex.europa.eu/eli/dir/2004/54/oj/eng>.
2. Italian Ministry of Infrastructures and Transports. Attuazione della direttiva 2004/54/CE in materia di sicurezza per le gallerie della rete stradale transeuropea [Internet]. [cited 2025 Apr 18]. Available from: <https://www.normattiva.it/uri-res/N2Ls?urn:nir:stato:decreto.legislativo:2006-10-05;264>. (In Italian).
3. Bonati A, Merusi F, Bochicchio G, Tessadri B, Polacco G, Filippi S, et al. Effect of nanoclay and conventional flame retardants on asphalt mixtures fire reaction. *Constr Build Mater*. 2023;47(6):990–1000. doi:10.1016/j.conbuildmat.2013.06.002.
4. Caliendo C, Russo I. CFD Simulation to assess the effects of asphalt pavement combustion on user safety in the event of a fire in road tunnels. *Fire*. 2024;7(6):195. doi:10.3390/fire7060195.
5. Xia W, Dong M, Xu T. Synergistic suppressions of porous warm mix agent and composite flame retardant on combustion and fume release of asphalt pavement. *J Clean Prod*. 2024;443(7):141003. doi:10.1016/j.jclepro.2024.141003.
6. Qin X, Zhu S, Chen S, Deng K. The mechanism of flame and smoke retardancy of asphalt mortar containing composite flame retardant material. *Constr Build Mater*. 2013;41(2):852–6. doi:10.1016/j.conbuildmat.2012.12.048.
7. Bi QQ, Li YM, He L, Wang DY. Fabrication of fire-retarded epoxy asphalt composites with compatibilization and toughening for road tunnel pavements. *Polym Degrad Stab*. 2024;229(2):110968. doi:10.1016/j.polymdegradstab.2024.110968.
8. Zhao Y, Wang Y, Wang M, Liang N, Li Z. Bio-mediated MOF-derived core-shell flame retardant: towards styrene-butadiene–styrene asphalt with enhanced flame safety and pavement performance. *Constr Build Mater*. 2023;392(7):131408. doi:10.1016/j.conbuildmat.2023.131408.
9. Sun M, He Z, Wu Y, Sun D, Fang K. Inhibitory effects of surface modified solid acid synergistic warm-mixed flame retardant on asphalt combustion behavior. *Constr Build Mater*. 2025;465(5):140266. doi:10.1016/j.conbuildmat.2025.140266.
10. Qian G, Yu H, Gong X, Zheng W. Effect of phosphorus slag powder on flammability properties of asphalt. *J Mater Civ Eng*. 2019;31(11):1104019280. doi:10.1061/(ASCE)MT.1943-5533.0002951.
11. Sheng Y, Ahmed AT, Jia H, Wu Y, Guo P, Li Y, et al. Preparation and characterization of low flammable asphalt for tunnel pavements. *Constr Build Mater*. 2022;359(7):129559. doi:10.1016/j.conbuildmat.2022.129559.
12. Wu K, Zhu K, Kang C, Wu B, Huang Z. An experimental investigation of flame retardant mechanism of hydrated lime in asphalt mastics. *Mater Des*. 2016;103(2):223–9. doi:10.1016/j.matdes.2016.04.057.
13. Li X, Zhou Z, Deng X, You Z. Flame resistance of asphalt mixtures with flame retardants through a comprehensive testing program. *J Mater Civil Eng*. 2017;29(4):04016266. doi:10.1061/(ASCE)MT.1943-5533.0001788.
14. Tan Y, He Z, Li X, Jiang B, Li J, Zhang Y. Research on the flame retardancy properties and mechanism of modified asphalt with halloysite nanotubes and conventional flame retardant. *Materials*. 2020;13(20):4509. doi:10.3390/ma13204509.
15. Yang X, Shen A, Liang M, Jiang Y, Meng Y. Dynamic flame retardancy and flame mechanism of SBS-modified asphalt containing alumina trihydrate and organic montmorillonite. *Constr Build Mater*. 2021;309(10):125077. doi:10.1016/j.conbuildmat.2021.125077.
16. Gupta R, Singh MK, Mavinkere Rangappa S, Siengchin S, Dhakal HN, Zafar S. Recent progress in additive inorganic flame retardants polymer composites: degradation mechanisms, modeling and applications. *Heliyon*. 2024;10(21):e39662. doi:10.1016/j.heliyon.2024.e39662.

17. Singh AP, Singh MK, Rangappa SM, Siengchin S, Pathak H, Zafar S. Addition of ammonium polyphosphate for simultaneous enhancement of flame retardancy, mechanical, and viscoelastic properties of PALF-reinforced bio-HDPE composite. *J Vinyl Addit Technol.* 2025;31(3):505–17. doi:10.1002/VNL.22185.
18. McGrattan K, Hostikka S, Floyd J, McDermott R, Vanella M. Fire dynamics simulator: user's guide. 6th. Gaithersburg, MD, USA: National Institute of Standards and Technology; 2019. 105 p.
19. Korhonen T. Fire dynamic simulator with evacuation: FDS + Evac—technical reference and user's guide. Espoo, Finland: VTT Technical Research Centre of Finland; 2018. 93 p.
20. Caliendo C, Russo I, Genovese G. Risk analysis of one-way road tunnel tube used for bi-directional traffic under fire scenarios. *Appl Sci.* 2021;11(7):3198. doi:10.3390/app11073198.
21. Caliendo C, Ciambelli P, De Guglielmo ML, Meo MG, Russo P. Computational analysis of fire and people evacuation for different positions of burning vehicles in a road tunnel with emergency exits. *Cogent Eng.* 2018;5(1):1530834. doi:10.1080/23311916.2018.1530834.
22. National Research Council. HCM 2010: highway capacity manual. Vol. 2. Washington, DC, USA: Transportation Research Board; 2010. 358 p. ISBN: 9788578110796.
23. Schrefler BA, Brunello P, Gawin D, Majorana CE, Pesavento F. Concrete at high temperature with application to tunnel fire. *Comput Mech.* 2002;29(1):43–51. doi:10.1007/s00466-002-0318-y.
24. Bonati A, Rainieri S, Bochicchio G, Tessadri B, Giuliani F. Characterization of thermal properties and combustion behaviour of asphalt mixtures in the cone calorimeter. *Fire Saf J.* 2015;74(6):25–31. doi:10.1016/j.firesaf.2015.04.003.
25. DiNenno PJ, Drysdale D, Beyler CL, Douglas Walton W, Custer RLP, Hall JR, et al. SFPE handbook of fire protection engineering. 3rd ed. Quincy, MA, USA: National Fire Protection Association; 2002. 1604 p.
26. Haack A. FIT-European thematic network fire in tunnels. Design fire scenarios; technical report part 1. Brussels, Belgium: European Commission; 2005. 161 p.
27. Xue H, Ho JC, Cheng YM. Comparison of different combustion models in enclosure fire simulation. *Fire Saf J.* 2001;36(1):37–54. doi:10.1016/S0379-7112(00)00043-6.
28. Yao H, Li Y, Lv K, Wang D, Zhang J, Zhan Z, et al. Numerical simulation analysis of the transformer fire extinguishing process with a high-pressure water mist system under different conditions. *Comput Model Eng Sci.* 2023;136(1):733–47. doi:10.32604/cmesci.2023.022155.
29. Avenel R, Demouge F, Fromy P. Fire behaviour study of asphalt road pavement in tunnel. In: Proceedings of the 10th International Conference on Fire and Materials; 2007 Jan 29–31; San Francisco, CA, USA.
30. National Fire Protection Agency. NFPA 502: standard for road tunnels, bridges, and other limited access highways. Quincy, MA, USA, 2020. 78 p. ISBN: 9781455923410.
31. CFPA Europe. Fire safety engineering concerning evacuation from buildings. Guidelines No. 19:2009 F [Internet]. [cited 2025 Apr 18]. Available from: https://cfpa-e.eu/app/uploads/2022/05/CFPA_E_Guideline_No_19_2009.pdf.